Online Supplemental Materials

MicroRNA miR-27b Rescues Bone Marrow-Derived Angiogenic Cell Function and Accelerates Wound Healing in Type 2 Diabetes

Jie-Mei Wang, Jun Tao, Dan-Dan Chen, Jing-Jing Cai, Kaikobad Irani, Qinde Wang, Hong Yuan, Alex F. Chen

Department of Surgery (JMW, DDC, QDW, AFC.), University of Pittsburgh School of Medicine, Pittsburgh, PA; Vascular Surgery Research (AFC), Veterans Affairs Pittsburgh Healthcare System, Pittsburgh, PA; Department of Hypertension & Vascular Disease (JMW, JT), First Affiliated Hospital of Sun Yat-Sen University, Guangzhou, China; Department of Cardiology and Center of Clinical Pharmacology (JMW, DDC,JJC, HY, QDW, AFC), Third Xiangya Hospital, Central South University, Changsha, Hunan, China; Division of Cardiovascular Medicine (KI), Department of Internal Medicine, University of Iowa Carver College of Medicine, Iowa City, IA.

JMW and JT contributed equally to this work

Running title: miR-27b augments bone-marrow derived angiogenic cell function in diabetes.

Address correspondence to:

Alex F. Chen, MD, PhD, FAHA

The Third Xiangya Hospital and the Institute of Vascular Disease and Translational Medicine, Central South University

138 Tong Zi Bo Road

Changsha, Hunan 410013 China

E-mail: afychen@yahoo.com

Supplemental Figure I. Phenotype of bone-marrow derived angiogenic cells (BMACs).

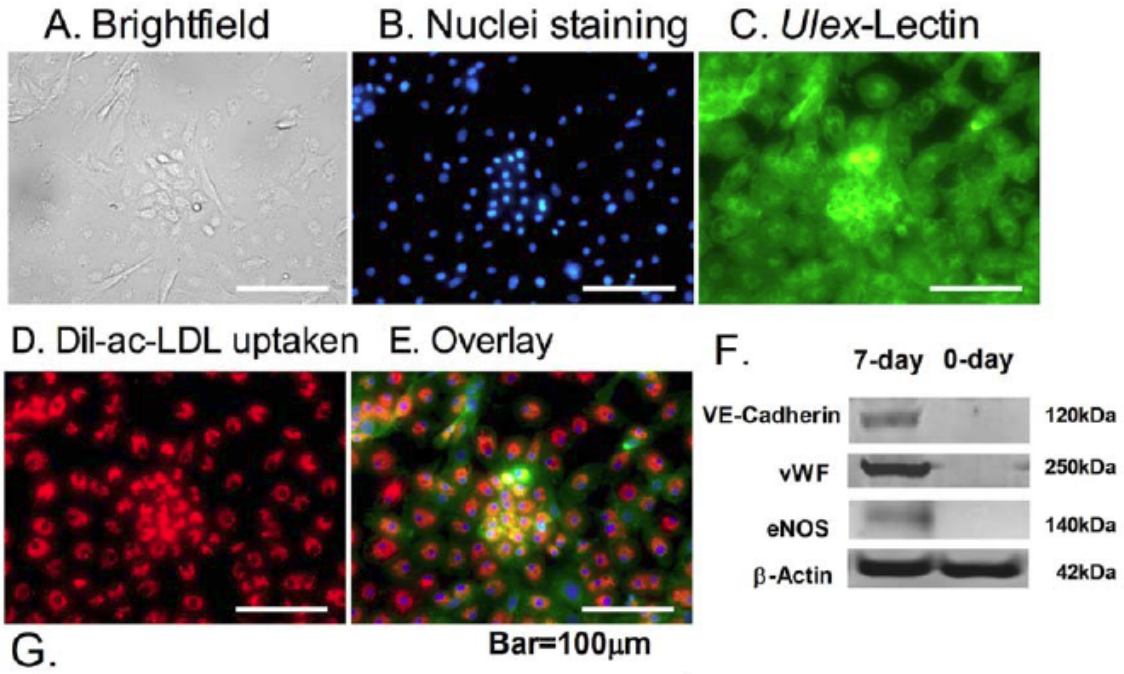

G.

Percentage	7-day			0-day		
Sca-1	65.16	±	3.16	14.91	±	2.01
CD34	45.72	±	3.86	22.08	±	1.06
FLK-1	20.77	±	1.76	3.37	±	0.49
CD144	8.33	±	1.14	1.97	±	0.24
Sca-1/Flk	15.85	±	0.88	3.4	±	0.67

After seven days in culture, BMACs presented spindle-shaped and cobblestone-like appearances (**A**). Fluorescent immunocytochemical staining showed that the adherent cells as their nuclei stained by Hoechst (**B**) were double positive (**E**) for *Ulex*-Lectin binding (**C**) and Dil-ac-LDL uptake (**D**), both of which are featured characteristics of endothelial lineage. Western Blot analysis indicated that seven-day cultured cells expressed VE-Cadherin, vWF, and eNOS (**F**). Flow cytometry analysis on BMACs cultured for seven days showed increased percentages of Sca-1, CD34, Flk-1, VE-Cadherin(CD144), and Sca-1/Flk-1 compared with freshly isolated mononuclear cells (**G**), suggesting that these cells are enriched for angiogenic cells.

Supplemental Figure II. TSP-1 protein expression was suppressed by miR-27b inhibitor, TSP-1 siRNA or both.

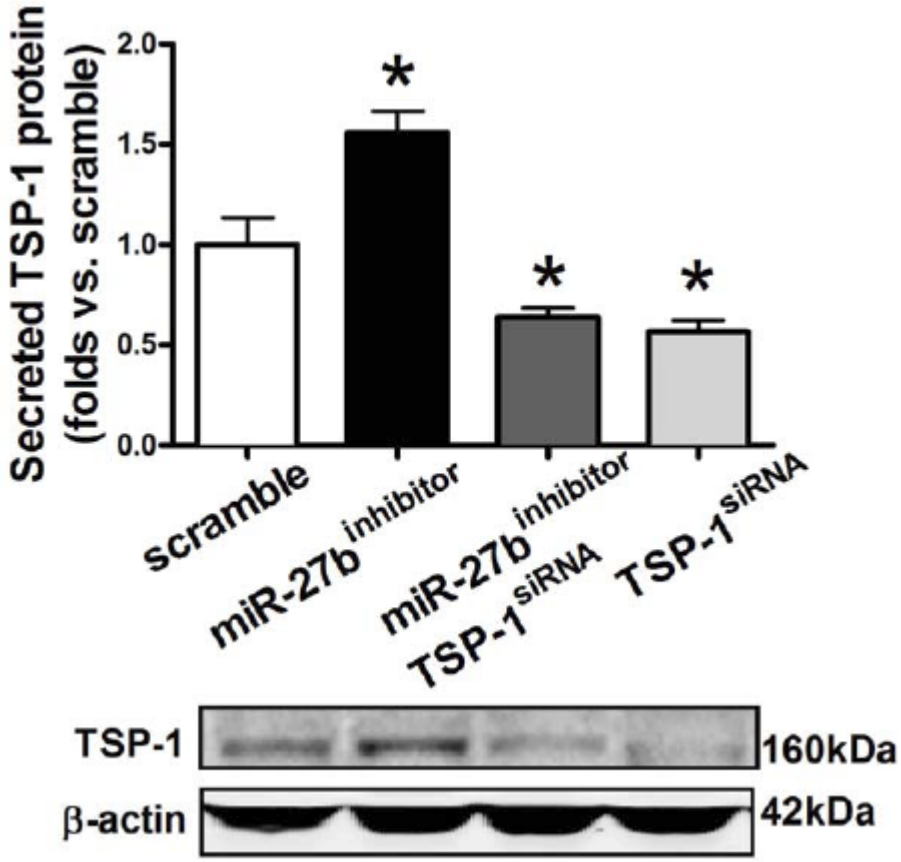

We detected TSP-1 protein expression after TSP-1 siRNA transfection and miR_27b inhibitor transfection, which was 120 hours of total transfection time. Our results demonstrated that the protein expression of TSP-1 was low in miR-27b inhibitor + TSP-1 siRNA group and TSP-1 siRNA groups, while it was high in miR-27b inhibitor group. The function of these cells were then evaluated by Matrigel tube formation shown in Figure 2F. Representative bands of TSP-1 were shown at button of the each bar graph. * $p<0.05$ vs. db/+ BMACs with scramble.

Supplemental Figure III. Sema6A but not Sprouty2 mediates the effects of miR-27b on BMAC proliferation.

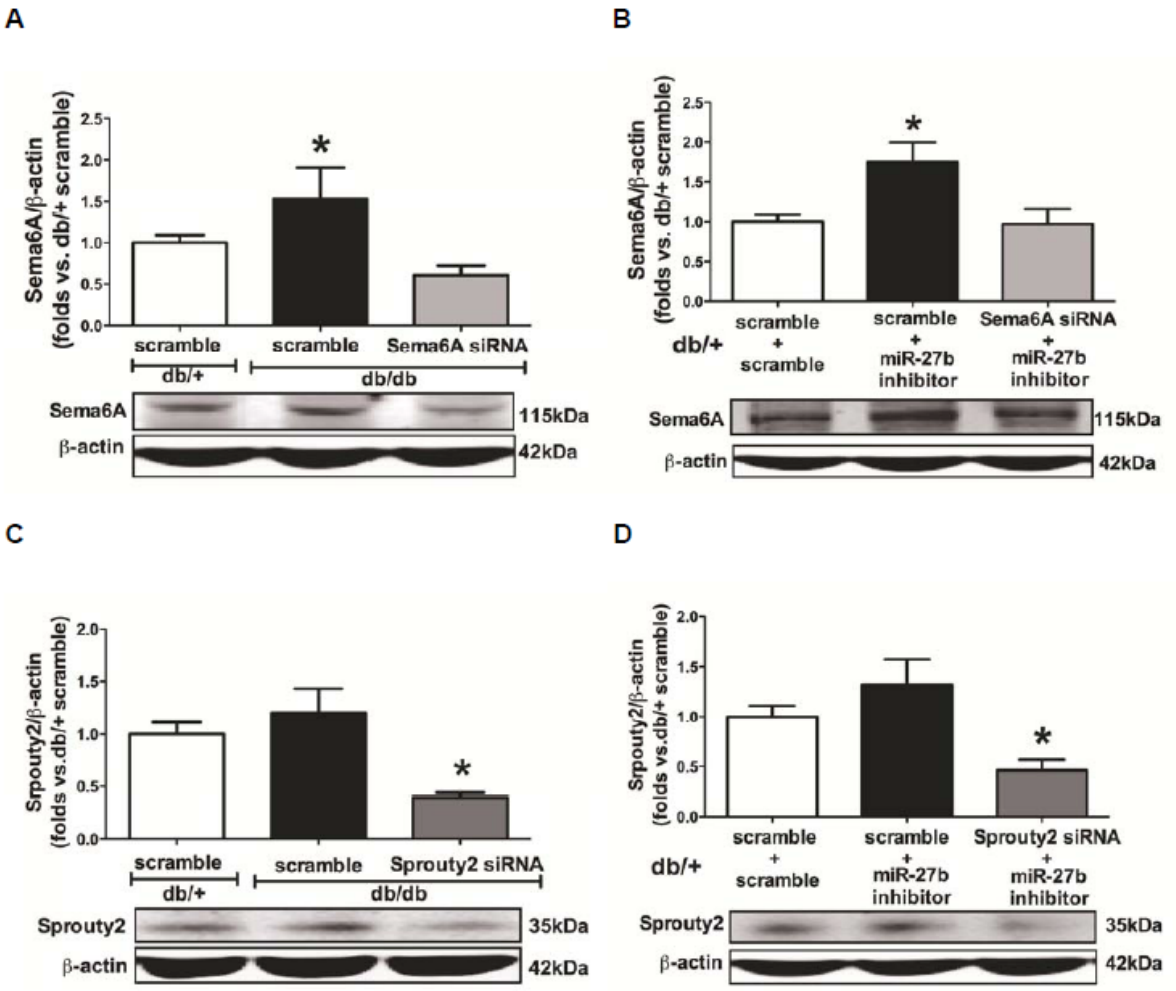

A. Protein expression of Sema6A in db/db BMACs with Scramble or Sema6A siRNA, using db/+ with scramble as controls. n=5, *p<0.05 vs. db/+ with scramble, # p<0.05 vs. db/db with scramble. **B.** Protein expression of Sema6A in db/+ BMACs with miR-27b inhibitor plus Sema6A siRNA. n=5, *p<0.05 vs. db/+ with scramble, # p<0.05 vs. db/db with scramble. **C.** Protein expression of Sprouty2 in db/db BMACs with Scramble or Sprouty2 siRNA, using db/+ with scramble as controls. n=5, *p<0.05 vs. db/+ with scramble, # p<0.05 vs. db/db with scramble. **D.** Protein expression of Sprouty2 in db/+ BMACs with miR-27b inhibitor plus Sprouty2 siRNA. n=5, *p<0.05 vs. db/+ with scramble, # p<0.05 vs. db/db with scramble.

Supplemental Figure IV. miR-27b and TSP-1 expressions in BMACs used for cell therapy.

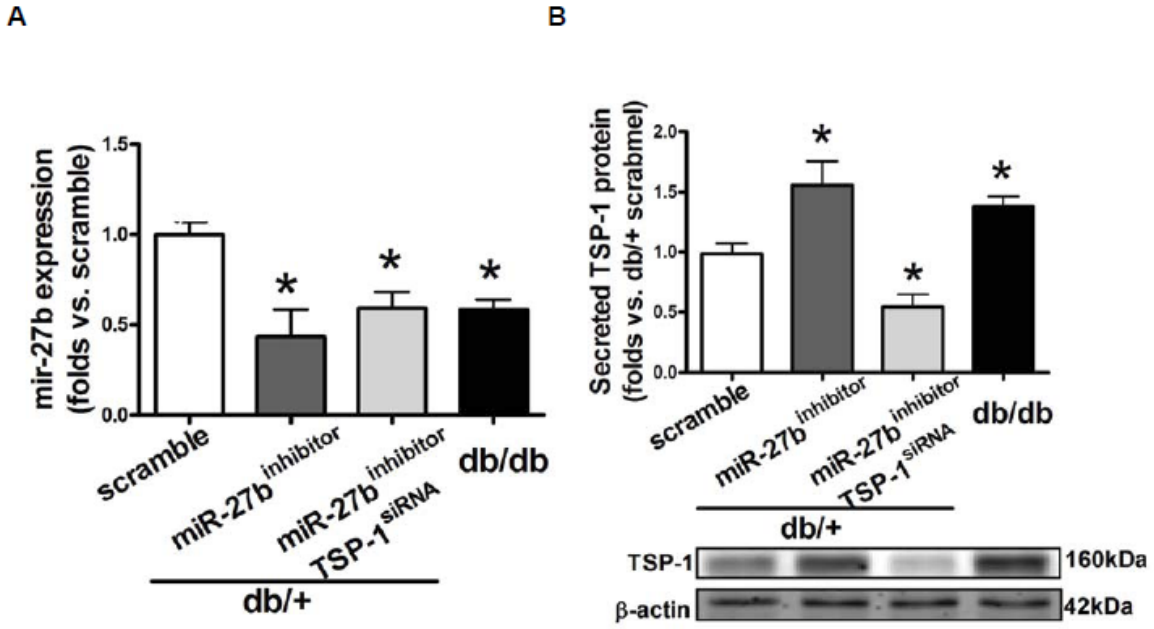

A. miR-27b expression in BMACs in each group by real-time PCR. n=4,* p<0.05 vs. db/+ BMACs+ scramble oligo. **B.** Secreted TSP-1 protein from BMACs in each group by Western blot. n=3,* p<0.05 vs. db/+ BMACs+ scramble oligo. Representative bands were shown at button of the bar graph.

Supplemental Figure V. Wound capillary formation after treatment.

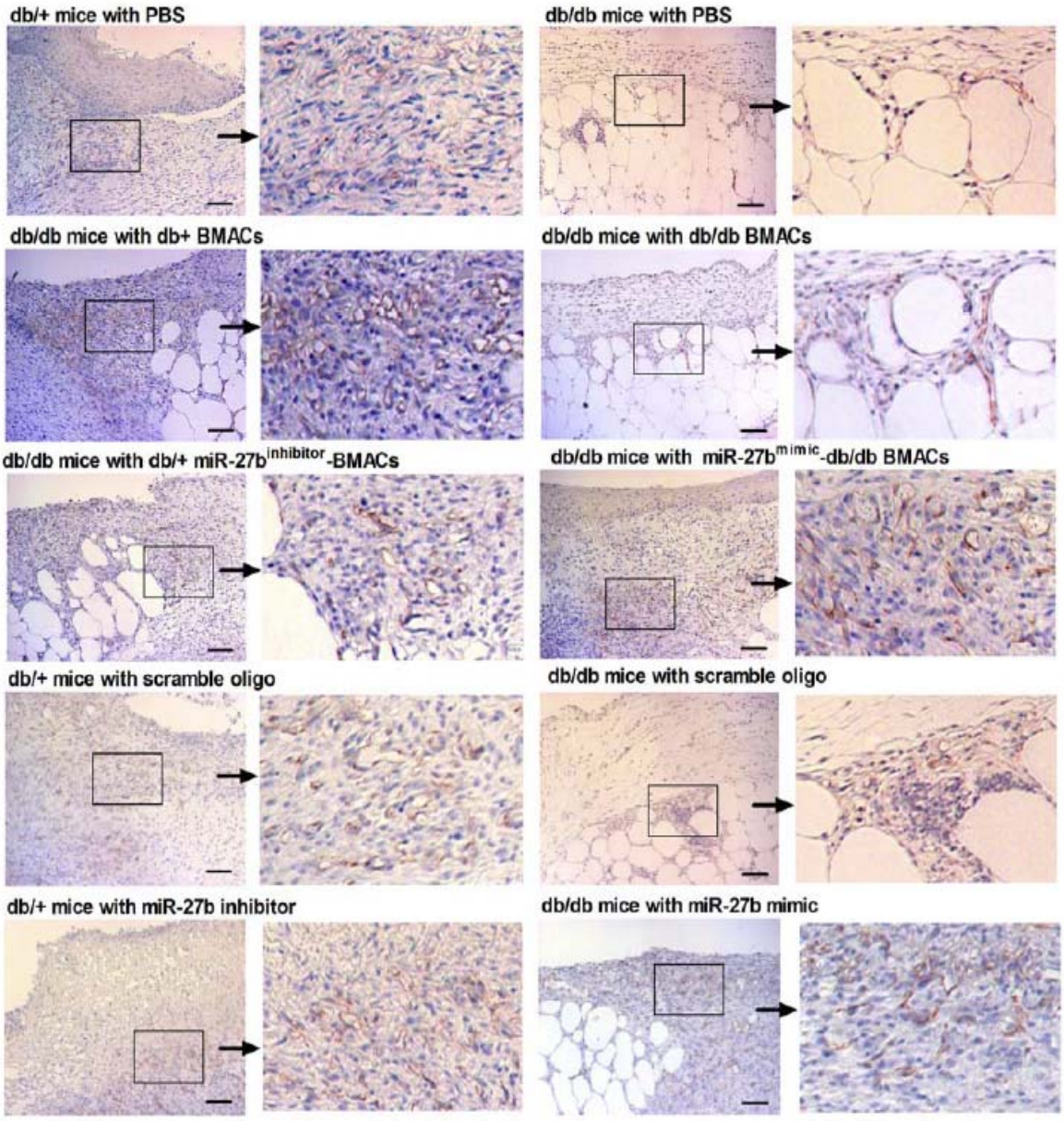

Typical photographs of CD31 staining on day 6 of wound healing. Boxed regions are shown at higher magnification to the right. CD31 positive cells were stained in brown color. Bar=100μm.

Supplemental Figure VI. miRNA expressions in BMACs from type 2 diabetic mice and normal mice.

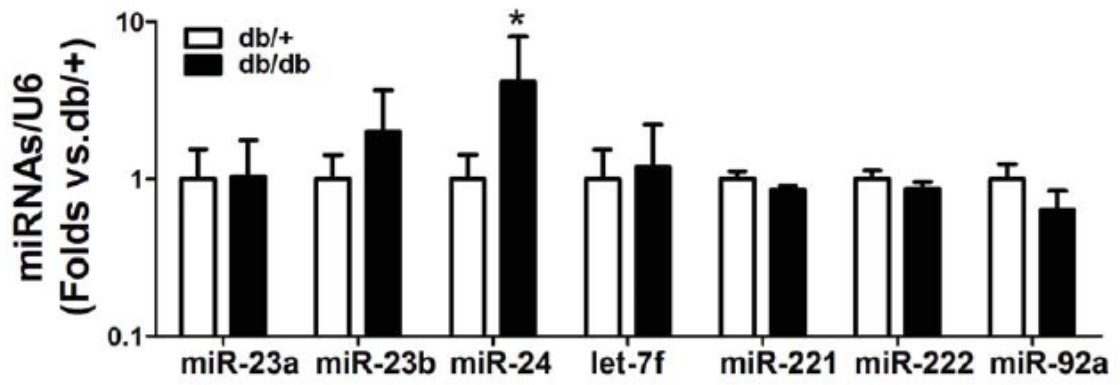

We detected some miRNAs within miR-23~24~27 clusters and angiogenesis-related miRNAs using real-time PCR. These miRNAs were miR-23a, miR-23b, miR-24, let-7f, miR-221, miR-222, and miR-92a. Our results demonstrated that miR-24 was increased in diabetic BMACs (Fig 2). The expressions of miR-23a, miR-23b, miR-24, let-7f, miR-221, miR-222 and miR-92a did not differ between diabetic and normal BMACs. miRNA expressions were detected by real-time PCR. n=6, *$p<0.05$ vs. db/+.

Supplemental Figure VII. TSP-1 mRNA is elevated in db/db BMACs, which is suppressed by miR-27b. Knocking down TSP-1 improves BMAC tube formation.

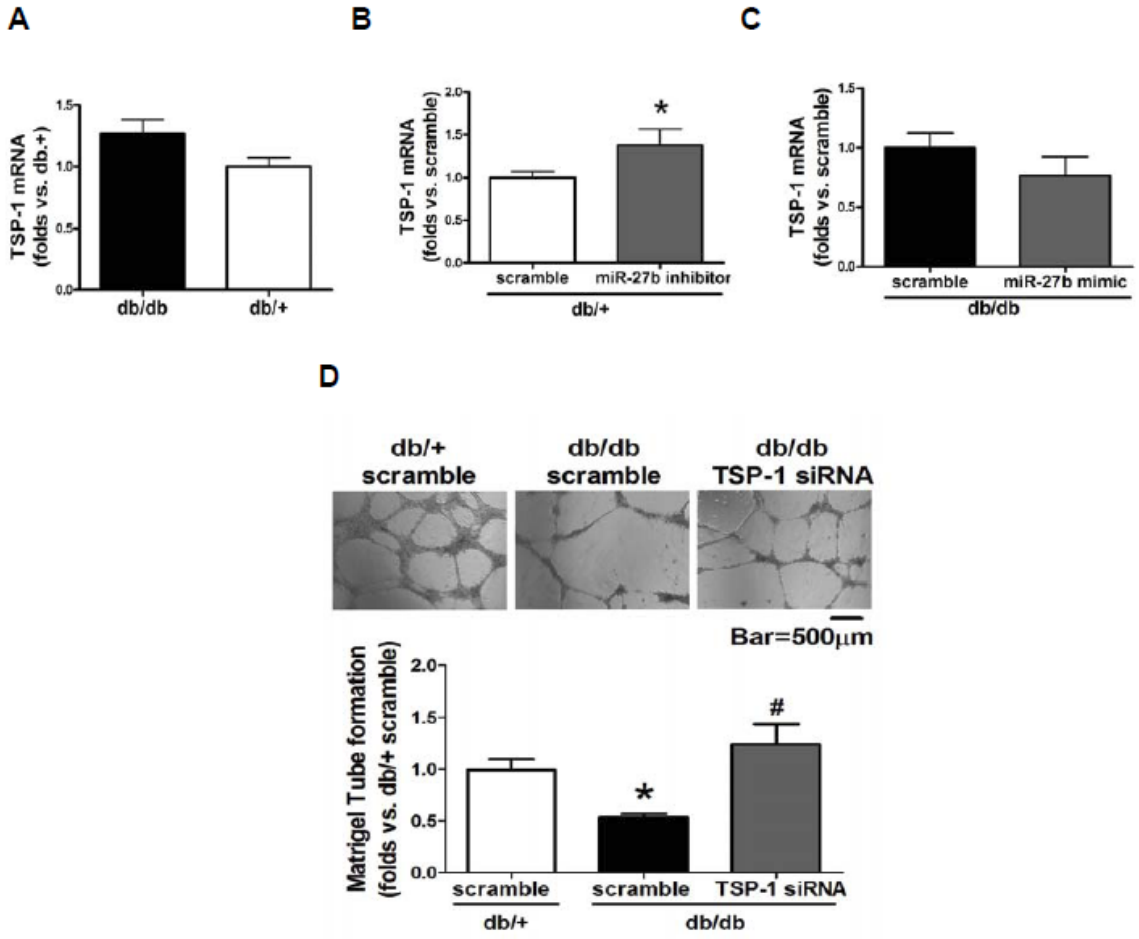

A.TSP-1 mRNA expression from db/+ and db/db BMACs. n=4, * p<0.05 vs. db/+ BMACs. **B**. TSP-1 mRNA expression of db/db BMACs with scramble or miR-27b mimic. n=4,* p<0.05 vs. Scramble. **C.** TSP-1 mRNA expression of db/+ BMACs with scramble or miR-27b inhibitor. n=4,* p<0.05 vs. Scramble. **D.** Matrigel tube network of db/db BMACs with TSP-1 siRNA or scramble, using db/+ BMACs with scramble as controls. n=6, *p<0.05 vs. db/+ with scramble. # p<0.05 vs. db/db with scramble.

Supplemental figure VIII. The effects of miR-27b on keratinocyte functions and mitochondrial oxidative status.

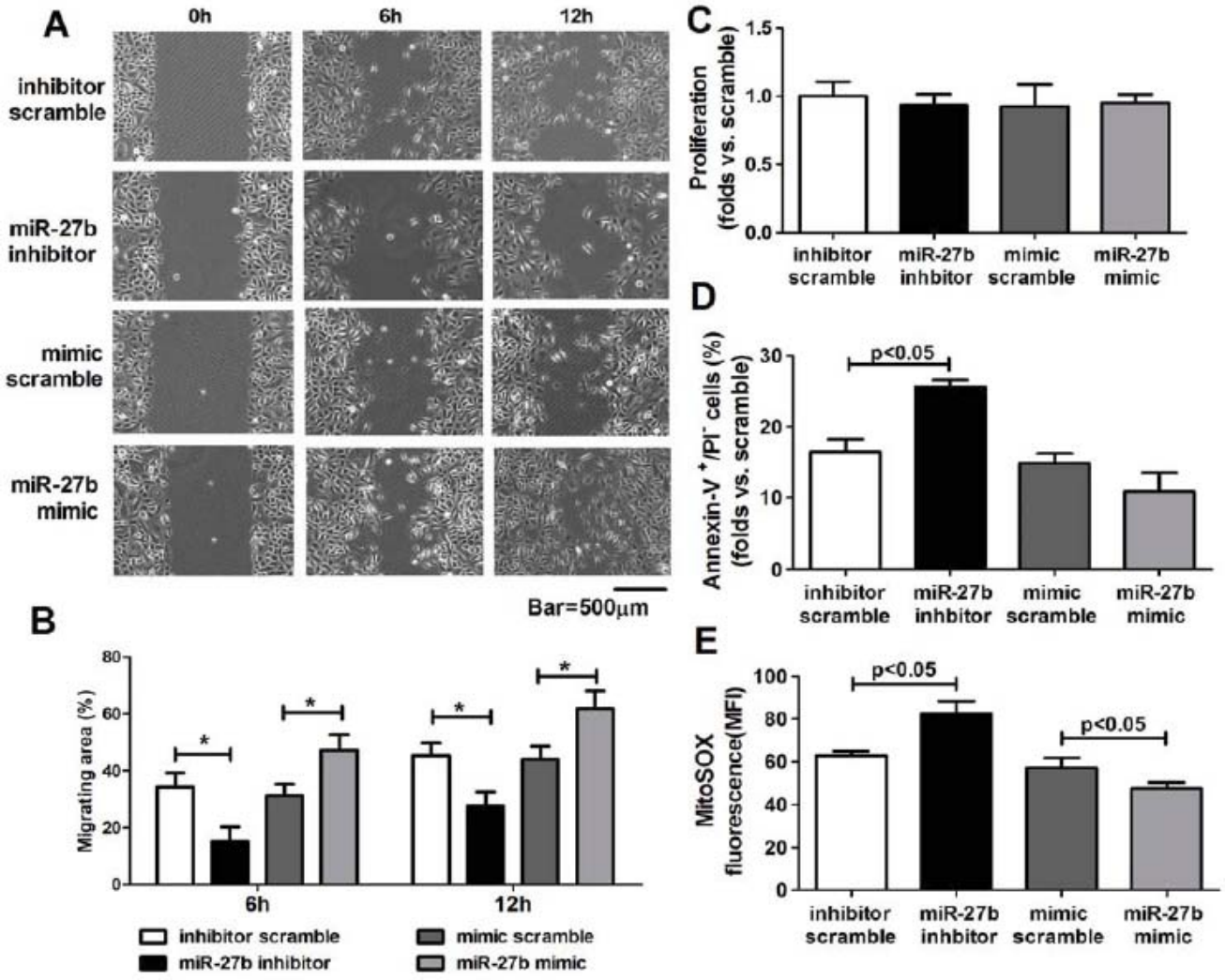

To determine whether miR-27b regulates keratinocyte functions, we evaluated migration, proliferations and apoptosis of keratinocytes after miR-27b manipulation. Human primary epidermal keratinocytes were transfected with miR-27b mimic or inhibitor or their scramble controls before tests. Our results demonstrated that miR-27b over-expression improved keratinoctye migration, while miR-27b inhibition impaired keratinoctye migration. **A.** representative pictures of migrating keratinocytes in scratch assay. **B.** Bar graph of migrating areas of keratinocytes six hours and 12 hours after scratch. * $p<0.05$ among two groups. **C.** The proliferation was not affected by miR-27b. There was no significant statistical difference among four groups. **D.** miR-27b inhibition increased keratinocyte apoptosis, but miR-27b over-expression did not show significant reduction in apoptosis. Bar graph shows Annexin-V^+/PI^- keratinocytes after miR-27b mimic/inhibitor transfection. **E.** miR-27b inhibition increased keratinocyte mitochondrial ROS, whereas miR-27b over-expression decreased mitochondrial ROS. Bar graph shows Mitochondrial ROS as stained by MitoSOX in keratinoctyes after miR-27b mimic/inhibitor transfection.

MicroRNA miR-27b rescues bone marrow-derived angiogenic cell function and accelerates wound healing in type 2 diabetes.

Jie-Mei Wang, Jun Tao, Dan-Dan Chen, Jing-Jing Cai, Kaikobad Irani, Qinde Wang, Hong Yuan, Alex F. Chen

Department of Surgery (JMW, DDC, QDW, AFC), University of Pittsburgh School of Medicine, Pittsburgh, PA; Vascular Surgery Research (AFC), Veterans Affairs Pittsburgh Healthcare System, Pittsburgh, PA; Department of Hypertension & Vascular Disease (JMW, JT), First Affiliated Hospital of Sun Yat-Sen University, Guangzhou, China; Department of Cardiology and Center of Clinical Pharmacology (JMW, DDC,JJC, HY, QDW, AFC), Third Xiangya Hospital, Central South University, Changsha, Hunan, China; Division of Cardiovascular Medicine (KI), Department of Internal Medicine, University of Iowa Carver College of Medicine, Iowa City, IA.

Materials and Methods

Animals

The db/db (BKS.Cg-m$^{+/+}$Lepr^{db}/J) mouse is a well-established diabetic animal model, demonstrating multiple vascular dysfunction and delayed wound healing similar to the condition found in patients with type 2 diabetes.[1] Male diabetic mice (db/db, age=10-12 weeks, plasma glucose 389.24±45.67 mg/dL) and their age- and gender-matched non-diabetic healthy littermates (db/+, BKS.Cg-m$^{-/-}$ Lepdb/$^{-}$ lean, plasma glucose 168.36±25.89 mg/dL) were purchased from The Jackson Laboratory (Bar Harbor, ME). CD47 global knockout (CD47$^{-/-}$,C57BL/6 background) and wildtype (C57BL/6) were from Jackson Laboratory. CD36 knockout (CD36$^{-/-}$, C57BL/6 background) mice were in-house colony in Department of Surgery at University of Pittsburgh. The animals were maintained under controlled environmental condition (12h: 12h light/dark cycle, temperature approximately 25°C), and provided with standard laboratory food and water *ad libitum*. All animal procedures were performed according to University of Pittsburgh Institutional Animal Care and Use Committee (IACUC) guidelines.

Human subjects

Six Type 2 diabetic patients with newly confirmed diagnosis (male=3, female=3,age=56±6.3 years, fasting glucose=9.4±1.8mmol/l) and five healthy age-matched volunteers (male=1, female=4, age=54±1.8 years, fasting glucose=5.1±0.5mmol/l) were recruited based on published criteria.[2] All the participants have acquired the nature of this study and given their written informed consent forms for the study, which was approved by the Ethics Committee of our hospital. Mononuclear cells were isolated from peripheral blood (20mL) by density gradient centrifugation and cultured using the same method described in online supplement [3, 4]. All the processes were performed by a single operator who was unaware of the subjects' state. Circulating angiogenic cells were cultured for 7 days and harvested for miR-27b detection.

BMAC *in vitro* culture and profiles

In vitro expansion of BMACs was performed as described in our recent reports.[3, 4] Bone marrow

mononuclear cells from the tibias and femurs of mice were plated on a culture flask coated with rat plasma vitronectin (Sigma-Aldrich) and maintained in Endothelial Growth Media (EGM-2, Lonza) in 37°C, 5% CO2 for seven days. On day 4 in culture, non-adherent cells were washed away. New medium was applied. After seven days in culture, to test the BMAC phenotype, attached cells were labeled with 1,1`-dioctadecyl-3,3,3`,3`- tetramethylindo- carbocyanine perchlorate-labeled acetylated LDL (Dil-ac-LDL, 1μg/ml, Sigma) and FITC-labeled Ulex europeus agglutinin (Ulex-Lectin, 1μg/ml; Sigma) for one hour. After nuclei staining by Hoechst 33258 (5μg/ml, Invitrogen), the samples were viewed with an inverted fluorescent microscope (Nikon). Pictures were taken in 200× high power fields. Cells demonstrating double-positive fluorescence of Dil-ac-LDL and Ulex-Lectin were identified as differentiating BMACs. Endothelial functional molecules including von Willebrand Factor (vWF), Vascular Endothelium Cadherin (VE-Cadherin) and endothelial nitric oxide synthase (eNOS) were detected using Western blot (please see “Western Blot Analysis” for details). In addition, the expression of stem cell markers such as Sca-1, CD34 and endothelial lineage markers such as Flk-1 and VE-Cadherin (CD144) were analyzed by flow cytometry and compared with freshly isolated bone marrow mononuclear cells. Adherent cells were gently detached using 5 mM EDTA/PBS at 37ºC, washed, and incubated for one hour on ice in PBS/0.5% (w/v) BSA together with FITC-labeled mouse antibodies (Abs) against Sca-1(1μg/10^6 cells, BD Bioscience), PE-labeled mouse Abs against Flk-1 (0.5μg/10^6 cells, BD Bioscience), FITC-labeled mouse Abs against CD34 (1μg/10^6 cells, BD Bioscience), PE-labeled mouse Abs against CD11b (0.5μg/10^6 cells, BD Bioscience), or their corresponding isotypic control Abs, respectively. To detect VE-Cadherin, cells were incubated with goat anti-mouse VE-cadherin Abs (2.5 μg/10^6 cells; R&D Systems) on ice for 20 minutes and then labeled with rabbit anti-goat Alexa 488 Abs (0.625 μg/10^6 cells; R&D Systems) on ice for 20 minutes. As staining control, 0.5% goat serum was used, followed by identical secondary antibody staining. Flow cytometry was performed using FACScan system and analyzed with Cell Quest software (BD Bioscience). Each analysis included at least 10,000 events.

Small interfering RNA and Mimic/Inhibitor Transfection

In vitro expansion of BMACs was performed as described in our recent reports.[3, 4] For small interfering RNA (siRNA)-mediated gene knockdown, BMACs after 7 days in culture were replanted at a density of 2.5×10^4 to $3.5\times10^4/cm^2$. SiRNA duplexes were transfected into BMACs with DharmaFECT transfection reagent I (all from Dharmacon), according to the protocol of the manufacturer. For over-expression or inhibition of miR-27b, BMACs were transfected with its specific mimic or inhibitor, 2'-O-Methyl oligoribonucleotides against miR-27b synthesized by Dharmacon (100nM), with DharmaFECT transfection reagent I (Dharmacon) according to the protocol of the manufacturer. In each experiment, non-related scramble oligo was used as a negative control. After 60 hours of silencing RNA and mimic/inhibitor transfection, the cells were harvested for the *in vitro* and *in vivo* experiments. In some experiments, db/+ BMACs were transfected with miR-27b inhibitor and/or siRNAs. First, transfection of siRNA or non-target siRNA (scramble, 100nM) was performed for 48-60 hours. Medium was changed. Second, transfection of miR-27b inhibitor or scramble oligo (100nM) was performed for 48-60 hours. The protein expression of target molecule was determined by western blot.

Quantitative Real-Time Polymerase Chain Reaction

Total RNA from BMACs were isolated by mirVanaTM miRNA Isolation Kit (Ambion) and collected as large RNA (for TSP-1 mRNA detection) and small RNA (for miR-27b detection). [3] For mRNA expressions, primers were as follows: TSP-1 forward ACT GGT GAA GGG CCA AGA TCT, reverse: 5'-GGA TCA GGT TGG CAT TCT CAA-3'; 18s (as internal control) forward: 5'-CGG GTC GGG AGT GGG T-3'; reverse: 5'-GAA ACG GCT ACC ACA TCC AAG-3'. Quantitative real-time PCR was performed using cDNA generated from 200ng of large RNA. For miR-27b detection, cDNA was generated from 10 ng of small RNA using specific reverse transcription primers for miR-27b synthesized by Ambion, Inc. Quantitative real-time PCR was performed using its specific real-time PCR primers synthesized by Amion, Inc. Amplification and detection of specific products were performed with the ABI PRISM 7500 Sequence Detection System with the cycle profile according to the protocol of mirVana qRT-PCR miRNA Detection Kit (Ambion, Inc), using sno55 as an internal control. Fluorescent signals were normalized to an internal reference, and the threshold cycle (C_t) was set within the exponential phase of the PCR. The relative gene expression was calculated by comparing cycle times for each target PCR. The miR-27b PCR C_t value was normalized by subtracting the sno55 C_t value, which gave the ΔC_t value. The relative expression levels of each target between groups were then calculated using the following equation: relative gene expression = $2^{-(\Delta Ct\_treatments-\Delta Ct\_controls)}$. [3]

Western Blot Analysis

Western blot analysis was performed by SDS/PAGE as we described previously.[5] For intracellular protein measurement, BMACs were lysed using Cell Lytic MT lysis buffer (Sigma) with Protease Inhibitor Cocktail (1:100 v/v, Sigma) for 20 minutes on ice. After centrifugation for 15 minutes at 12,000 *g* (4°C), the protein content of the samples was determined by BCA assay (Bio-Rad). For secreted TSP-1 or TSP-2 protein measurement, the culture medium was replaced with 2 ml of serum-free medium and the cells were incubated for 4 hours.[6] The conditioned medium of each sample was collected, concentrated with a Centricon-10 (Amicon, Danvers, MA), and protein concentrations were determined with the BCA assay. At the same time, all the BMACs of each sample were lysed to extract cytoplasmic protein for the detection of β-actin. The TSP-1 or TSP-2 levels in culture medium were normalized by β-actin. Equal amounts of protein (30μg) were loaded onto SDS/PAGE and blotted onto nitrocellulose membranes (Bio-rad). Immunobloting was performed by using antibodies directed against each target molecule: Akt (rabbit anti-mouse Akt, 1:1000; Cell signaling); phosphorylated- Akt^{ser473} (rabbit anti-mouse Akt, 1:1000; Cell signaling); eNOS (rabbit anti-mouse eNOS, 1:1000; Cell signaling), phosphorylated-$eNOS^{s1177}$ (rabbit anti-mouse eNOS, 1:1000; Cell signaling), TSP-1 (mouse monoclonal anti-TSP-1, 1:400 Abcam), TSP-2 (mouse monoclonal anti-TSP-2, 1:400; Abcam), $p66^{shc}$ (mouse anti-SHC, 1:1000; BD Biosciences),Sema6A (goat anti-mouse Semaphorin 6A, 1:500, R&D); Sprouty2 (rabbit anti-mouse Sprouty2, 1:1000, Abcam); MnSOD (mouse monoclonal anti-MnSOD,1:500, Abcam), Cu/ZnSOD (rabbit anti-mouse Cu/ZnSOD, 1:500, Abcam) and catalase (rabbit anti-mouse catalase,1:200, Santa Cruz), VEGF (rabbit anti-mouse VEGF,1:1000, Millipore), Angiopoietin-1 (rabbit anti-mouse Angiopoietin-1,1:500, Abcam),SDF-1α (rabbit anti-mouse SDF-1α,1:250, Santa Cruz), β-actin (mouse monoclonal anti-β-actin, 1:10000, Sigma, served as loading control). Secondary antibodies included IRDye 800–conjugated rat anti-mouse antibody (1:4000, Rockland), Alexa Fluor 680 goat anti-rabbit IgG antibody (1:2500, Rockland) and Alexa Fluor 800 donkey anti-goat IgG antibody (1:2500,

Rockland). The blot was read with an Odyssey imager (Li-Cor). Molecular band intensity was determined with Odyssey 2.1 software (Li-Cor).

BMAC Function Assays (Proliferation, Tube Formation, Migration, Adhesion, Apoptosis)

In tube formation assay, BMACs in EBM-2 plus 5% FBS were plated in a 48-well cell culture plate (5×10^4 cells per well) pre-coated with 150μl of growth factor-reduced Matrigel-Matrix (BD Biosciences) as described previously. [7] After 24-hour incubation, images of tube morphology were taken by inverted microscope (Nikon) at the magnification ×40 and tube lengths were measured at 5 random fields per well. In adhesion assay, BMACs were plated in a 96-well plates (2.5×10^4 cells per well) pre-coated with 2.5 g/ml vitronectin. After 1-hour incubation, non-adherent cells were washed away and adherent cells were fixed with 2% Paraformaldehyde. Nuclei were stained with Hoechst (5μg/L, Sigma) for 20 minutes. The number of adherent cells was counted at the magnification ×100, and the mean value of 4 wells was determined for each sample.[8] The migration assay was performed using a modified Boyden's chamber assay as described previously.[6] Around 5×10^4 BMACs were placed into upper Boyden's chamber with EBM-2 plus 5% FBS. The lower chamber was loaded with EBM-2 plus 5% FBS and VEGF (50ng/ml). BMACs were allowed to migrate for 24 hours. The cells remaining on the upper chamber were mechanically removed. Cells on the lower side of the membrane were fixed and stained with Hoechst, counted at magnification ×100. The mean value of 5 different fields was determined for each sample. Cell proliferation was evaluated by MTS assay using CellTiter 96® Aqueous One Solution Cell Proliferation Assay Kit (Promega). BMACs in EGM-2 were plated in a 96-well culture plate (1×10^4 cells per well) overnight before different treatments. After the treatments, cell were washed with pre-warmed E`BM-2 and100μl EGM-2 with 20μl assay aliquots were added. BMACs were cultured for 4 hours in 5% CO_2,37ºC. The absorbance was read at 490 nm in 100 μL of soluble formazan medium with a microplate spectrophotometer. Cell number was then calculated from a standard cure and expressed as folds of the controls. Cell apoptosis was evaluated with Annexin V-FITC/PI Apoptosis Detection Kit (Invitrogen). The cells were stained with Annexin-V-FITC and propidium iodide in 1 × binding buffer for 15 min at room temperature. Flow-cytometric analyses were performed on FACScan system and analyzed with Cell Quest software (BD Bioscience). Each analysis included at least 10,000 events.

Luciferase Reporter Assays of miR-27b to 3'UTR of Target mRNAs

The luciferase target assay was performed as previously described [9-11]. Synthetic oligonucleotides as indicated by NCBI reference sequence bearing either human TSP-1 (THBS1) mRNA 3'UTR (NM_003246), human TSP-2 (THBS2) mRNA 3'UTR (NM_003247.2), human $p66^{shc}$ (SHC1) mRNA 3'UTR(NM_183001.4), human Semaphorin 6A (Sema6A) mRNA 3'UTR (NM_020796), or Sprouty2 (SPRY2) mRNA 3'UTR (NM_005842) was cloned into pMirTarget plasmid after the stop codon of luciferase, respectively. The co-transfection of mutant sequence of each mRNA 3'UTR and miR-27b mimic served as controls. In this vector system, a red fluorescent protein (RFP) under a CMV promoter is used to monitor the transfection and normalizing transfection efficiency. For examples, HEK 293 cells (50% confluence in each well of 6-well plate) were co-transfected with 100ng of TSP-1 (THBS1) 3'UTR plasmid and 0.1nmol of miR-27b mimic (Dharmacon), all combined with Turbofect 8.0 (Origene) according to manufacture's protocol. As control, similar oligonucleotides to TSP-1 mRNA 3'UTR with mutant

miR-27b binding site was cloned into pMirTarget plasmids and co-transfected with miR-27b mimic (see below for mutant sequences). The same protocol was used to co-transfect other 3'UTR plasmid and miR-27b mimic. After 48 h, cells were washed and lysed with Reporter Lysis Buffer (Promega), and their luciferase activity was measured using the GloMax® 96 Microplate Luminometer (Promega). The relative reporter activity was obtained by normalization to each rmutant plasmid co-transfection. A reduced firefly luciferase activity indicated the direct binding of miR-27b to the cloned target sequence.

3'	CGUCUUGAAUCGGUGACACUU	5' hsa-miR-27b
1517: 5'	UUACCUCAUUUGUUGUGUGAC	3' THBS1(wildtype)
1517: 5'	UUACCUCAUUUGUUG**UUCA**AC	3' THBS1(mutant)
3'	CGUCUUGAAUCGGUGACACUU	5' hsa-miR-27b
1099:5'	AUAAGUAUAUAAUCCUGUGAA	3' THBS2(wildtype)
1099:5'	AUAAGUAUAUAAUCC**GAC**GAA	3' THBS2(mutant)
3'	CGUCUUGAAUCGGUGACACUU	5' hsa-miR-27b
1126: 5'	UUCCUCGCCUAGGCCUGUGAG	3' SHC1(wildtype)
1126: 5'	UUCCUCGCCUAGGCC**GAC**GAG	3' SHC1(mutant)
3'	CGUCUUGAAUCGGUGACACUU	5' hsa-miR-27b
555:5'	ACUAUGCGCAAAUACUGUGAA	3' Sema6A(wildtype)
555:5'	ACUAUGCGCAAAUAC**CAG**GAA	3' Sema6A(mutant)
3'	CGUCUUGAAUCGGUGACACUU	5' hsa-miR-27b
368:5'	CAAUAAUAUUUGCAACUGUGAA	3' SPRY2(wildtype)
368:5'	CAAUAAUAUUUGCAAC**CAG**GAA	3' SPRY2(mutant)

MitoSOX staining

The mitochondrial reactive oxygen species were detected using MitoSOX™ Red mitochondrial superoxide indicator (Invitrogen) as we previously described.[12] MitoSOX™ is a novel fluorogenic dye for highly selective detection of superoxide in the mitochondria of live cells. Once in the mitochondria, MitoSOX™ Red reagent is oxidized by superoxide and exhibits red fluorescence. BMACs were harvested after miR-27b mimic/inhibitor transfection and incubated in HBSS containing 5μM MitoSOX™ for 10 minutes. Immediately after the incubation, flow cytometry was performed using FACScan system and analyzed with Cell Quest software (BD Bioscience). Each analysis included at least 10,000 events.

Ad-p66^{shc}RNAi transfection

For p66^{shc} down-regulation, BMACs were transfected by recombinant adenovirus Ad-p66^{shc}RNAi at the titer of 10MOI, as established previously.[13] Dr. Kaikobad Irani kindly donated the virus. This adenovirus encodes a short hairpin loop RNA with a 19-mer sequence corresponding to bases 45–63 of the cDNA of p66^{shc} and is unique to mRNA of p66^{shc}.[14] Ad-β-gal was also used for internal control. Adenovirus transfection was performed in EGM-2 supplemented with 2% FBS for 24h, followed by change of EGM-2 with 5% FBS. Then miR-27b inhibitor transfection was performed for 60h, as described above.

Topical BMAC therapy on wound healing *in vivo*

Wounds were created on the dorsal surface of the mouse as previously described.[15] Full-thickness skins were removed using a 6-mm punch biopsy without hurting the underlying

muscle. In mice with BMAC therapy, 1×10^6 BMACs with different gene manipulation in 30 μl PBS were topically transplanted onto the wound area immediately after punch. The grouping was as follows: 1) db/+ wound with PBS; 2) db/db wound with PBS; 3) db/db wound with db/+ BMACs; 4) db/db wound with db/db BMACs; 5) db/db wound with db/db miR-27b^{mimic}-BMACs; 6) db/db wound with db/+ miR-27b^{inhibitor}-BMACs; 7) db/db wound with db/+ miR-27b^{inhibitor}TSP-1^{siRNA}-BMACs.

Wounds were covered with transparent oxygen-permeable wound dressing (Bioclusive, Johnson & Johnson). The dressings were changed every other day. Wound closure rates were measured by tracing the wound area onto acetate paper every other day until day 10. The tracings were digitized, and the areas were calculated with a computerized algorithm and converted to percent wound closure (Image J). Wound closure rates were calculated as Percentage Closed (y%) =[(Area on Day_0–Open Area on Day_x)/Area on Day_0]×100, as described previously .[16]

Laser Doppler imaging (LDI) using PeriScan PIM3 system (Perimed AB, Sweden) was performed to measure the perfusion of the wound areas immediately after wounding and every other day until day 16 as described previously.[17, 18] Low-intensity (0.20) laser beams (630nm) were used to scan across wound surface with fixed distance (20cm) from each wound site under standard room illumination. The scan area included the entire wound site and margins. In the following measurements, the same position, detection area, and distances were referred to the first detection profile gained from the same mouse. Blood flow measurements of the microvasculature were calculated with a 214 × 214 pixel resolution, with each pixel being an actual measurement of flux or blood flow (speed of blood cells × blood volume). Color-coded images representing the microvascular blood flow distribution were recorded. Low perfusion was displayed in dark blue and highest perfusion areas were displayed in red. Color images were analyzed by self-contained software Perimed LDPIwin 3.0. A circle was drawn to capture the original size of wound area and the mean perfusion data within this circle were expressed as perfusion index.

Local delivery of miR-27b inhibitor on normal wounds

The effect of topical miR-27b mimic/inhibitor transfection on normal wound healing was measured. An established model of local oligonucleotide delivery via F-127 pluronic gel was applied as previously described.[19] Excisional full-thickness cutaneous wounds were created in db/+ mice as described above. Briefly, 0.25 nmol of miR-27b inhibitor (equals to ~3.5 μg) was preloaded into the 10μl, 30% F-127 pluronic gel (Sigma) at 4°C. DharmaFECT transfection reagent I (Dharmacon) was added at a final concentration of 1% in F-127 pluronic gel loaded with miR-27b inhibitor. The gel was applied locally to the surface of wound area and absorbed within 2 hours. The procedure was repeated every other day from day 0 to day 8. The control wounds were treated with 1% F-127 pluronic gel loaded with 0.25 nmol of scramble oligo and 1% of DharmaFECT transfection reagent I. Wound closure rates and wound blood flow were monitored as described above. On day 6, some of wound samples were harvested for miR-27b expression using real-time PCR.

Wound capillary formation

Wounds were recovered from mice on Day6. Capillary density in the healing wounds was quantified by histological analysis. Wound samples were fixed with zinc chloride fixative (BD) for 24 hours, then embedded in paraffin, and sectioned at 4-μm intervals. Slides were deparaffinized and hydrated, then placed in Tris-Buffered Saline (pH 7.5) for 5 minutes for pH adjustment. Endogenous peroxidase was blocked by 3% Hydrogen Peroxide/Methanol bath for 20 minutes, followed by distilled H_2O rinses. Slides were blocked with normal rabbit serum (Vector Laboratories) for 30 minutes, then incubated for 60 minutes at room temperature with an anti-CD31 antibody (1:50; Santa Cruz), and further incubated with Vectastain Elite ABC Reagent (Vector Laboratories) for 30 minutes and Nova Red (Vector Laboratories) for 15 minutes. Slides were counterstained with Gill (Lerner) 2 Hematoxylin (VWR Scientific) for 10 seconds, differentiated in 1% aqueous glacial acetic acid, and rinsed in running tap water. Ten random microscopic fields (×200 magnification) were counted to determine the number of capillaries per wound. Pictures were taken under a Zeiss Axioskop microscope using Image-Pro Plus sofeware (Media Cybernetics).

BMAC Integration

BMACs were isolated as described above and cultured in EGM-2. BrdU staining was performed on BMACs. On day 5 of culture EPCs were labeled with 5-bromo-2'-deoxyuridine and 5-fluro-2'deoxyuridine (BrdU labeling reagent, Invitorgen). BrdU labeling reagent was diluted 1:100 in EGM-2, filtered through a 0.2 :m filter, and warmed to 37°C. 1 mL of BrdU/EGM-2 was added to cells in a 6 well plate and incubated overnight. The wells were washed 3 times with PBS followed by trypsinization to re-suspend the cells. a number of 1×10^6 BMACs were then transplanted to a db/db wound (6 mm punch biopsy) as described above. After 6 days of wound healing, the mouse was euthanized, and the wound and surrounding skin was recovered and fixed in 10% formalin for 24 hours. Slides were double-stained with an anti-CD31 antibody followed by BrdU antibody (1:50; Santa Cruz Biotechnology Inc.) incubation. Pictures were taken under a Zeiss Axioskop microscope using Image-Pro Plus sofeware (Media Cybernetics).

miR-27b mimic/inhibitor transfection on human primary epidermal keratinocytes

Human primary epidermal keratinocytes were purchased from ATCC and cultured in dermal cell basal medium supplemented with keratinocyte growth kit (ATCC) according to the manufacturer's protocol. For over-expression or inhibition of miR-27b, keratinocytes were transfected with its specific mimic or inhibitor, 2'-O-Methyl oligoribonucleotides against miR-27b synthesized by Dharmacon (100nM), with DharmaFECT transfection reagent I (Dharmacon) according to the protocol of the manufacturer. In each experiment, non-related scramble oligo was used as a negative control. After 60 hours of silencing RNA and mimic/inhibitor transfection, the cells were harvested for the *in vitro* experiments.

Migration, proliferation, and apoptosis of epidermal keratinocytes

Keratinocyte migration was tested in an *in vitro* scratch assay as previously described, with slight modification [20]. A number of 3×10^5 keratinocytes were seeded in six-well plates. After reaching 100% confluence, cells were washed twice with PBS and scratched using a pipette-tip. The resulting scratch was investigated under the microscope and the area for photographs was marked using a pen on the bottom of the well. Immediately after scratching, the first photograph was taken (initial wound size) exactly at the marked area.

After six hours and 12 hours, the same areas of the scratch wounds were photographed again and the reduction in wound width was measured using ImageJ 1.45 s software (National Institutes of Health, Bethesda, MD). Cell proliferation was evaluated by MTS assay using CellTiter 96® Aqueous One Solution Cell Proliferation Assay Kit (Promega). Keratinocytes in dermal cell basal medium were plated in a 96-well culture plate (1×10^4 cells per well) overnight before different treatments. After the treatments, cell were washed with pre-warmed E`BM-2 and 100µl EGM-2 with 20µl assay aliquots were added. Keratinocytes were cultured for four hours in 5% CO_2,37ºC. The absorbance was read at 490 nm in 100 µL of soluble formazan medium with a microplate spectrophotometer. Cell number was then calculated from a standard cure and expressed as folds of the controls. Cell apoptosis was evaluated with Annexin V-FITC/PI Apoptosis Detection Kit (Invitrogen). The cells were stained with Annexin-V-FITC and PI in 1 × binding buffer for 15 minutes at room temperature. Flow-cytometric analyses were performed on FACScan system and analyzed with Cell Quest software (BD Bioscience). Each analysis included at least 10,000 events.

Data Analysis

All values were expressed as mean±SEM. The statistical significance of differences between the 2 groups was determined with Mann-Whitney U nonparametric test. When more than two treatment groups were compared, one-way ANOVA followed by LSD post hoc testing was used.[21] For the *in vivo* wound closure data, two-way repeated measures ANOVA followed by Bonferroni post hot testing was used to compare both differences between treatments and time courses. For wound perfusion data, Receive Operating Characteristic (ROC) Curve Analysis was performed to compare the differences between treatments. In all tests, $p<0.05$ was considered statistically significant.

References:

1. Emanueli C, Caporali A, Krankel N, Cristofaro B, Van Linthout S, Madeddu P. Type-2 diabetic Lepr(db/db) mice show a defective microvascular phenotype under basal conditions and an impaired response to angiogenesis gene therapy in the setting of limb ischemia. *Front Biosci.* 2007;12:2003-2012.
2. Esposito K, Maiorino MI, Di Palo C, Gicchino M, Petrizzo M, Bellastella G, Saccomanno F, Giugliano D. Effects of pioglitazone versus metformin on circulating endothelial microparticles and progenitor cells in patients with newly diagnosed type 2 diabetes--a randomized controlled trial. *Diabetes Obes Metab.* 2010;13:439-445.
3. Zhao T, Li J, Chen AF. MicroRNA-34a induces endothelial progenitor cell senescence and impedes its angiogenesis via suppressing silent information regulator 1. *American journal of physiology.*299:E110-116.
4. Marrotte EJ, Chen DD, Hakim JS, Chen AF. Manganese superoxide dismutase expression in endothelial progenitor cells accelerates wound healing in diabetic mice. *J Clin Invest.* 2010;120:4207-4219.
5. Du YH, Guan YY, Alp NJ, Channon KM, Chen AF. Endothelium-specific GTP cyclohydrolase I overexpression attenuates blood pressure progression in salt-sensitive low-renin hypertension. *Circulation.* 2008;117:1045-1054.
6. Ii M, Takenaka H, Asai J, Ibusuki K, Mizukami Y, Maruyama K, Yoon YS, Wecker A, Luedemann C, Eaton E, Silver M, Thorne T, Losordo DW. Endothelial progenitor thrombospondin-1 mediates diabetes-induced delay in reendothelialization following arterial injury. *Circ Res.* 2006;98:697-704.
7. Luo JD, Hu TP, Wang L, Chen MS, Liu SM, Chen AF. Sonic hedgehog improves delayed wound healing via enhancing cutaneous nitric oxide function in diabetes. *Am J Physiol Endocrinol Metab.* 2009;297:E525-531.
8. Hamada H, Kim MK, Iwakura A, et al. Estrogen receptors alpha and beta mediate contribution of bone marrow-derived endothelial progenitor cells to functional recovery after myocardial infarction. *Circulation.* 2006;114:2261-2270.
9. Bonauer A, Carmona G, Iwasaki M, et al. MicroRNA-92a controls angiogenesis and functional recovery of ischemic tissues in mice. *Science.* 2009;324:1710-1713.
10. Felli N, Fontana L, Pelosi E, et al. MicroRNAs 221 and 222 inhibit normal erythropoiesis and erythroleukemic cell growth via kit receptor down-modulation. *Proceedings of the National Academy of Sciences of the United States of America.* 2005;102:18081-18086.
11. Petersen CP, Bordeleau ME, Pelletier J, Sharp PA. Short RNAs repress translation after initiation in mammalian cells. *Mol Cell.* 2006;21:533-542.
12. Wang XR, Zhang MW, Chen DD, Zhang Y, Chen AF. AMP-activated protein kinase rescues the angiogenic functions of endothelial progenitor cells via manganese superoxide dismutase induction in type 1 diabetes. *American journal of physiology. Endocrinology and metabolism.* 2011;300:E1135-1145.
13. Kim CS, Jung SB, Naqvi A, Hoffman TA, DeRicco J, Yamamori T, Cole MP, Jeon BH, Irani K. p53 impairs endothelium-dependent vasomotor function through transcriptional upregulation of p66shc. *Circulation research.* 2008;103:1441-1450.
14. Yamamori T, White AR, Mattagajasingh I, Khanday FA, Haile A, Qi B, Jeon BH, Bugayenko A, Kasuno K, Berkowitz DE, Irani K. P66shc regulates endothelial NO

production and endothelium-dependent vasorelaxation: implications for age-associated vascular dysfunction. *J Mol Cell Cardiol.* 2005;39:992-995.

15. Gallagher KA, Liu ZJ, Xiao M, Chen H, Goldstein LJ, Buerk DG, Nedeau A, Thom SR, Velazquez OC. Diabetic impairments in NO-mediated endothelial progenitor cell mobilization and homing are reversed by hyperoxia and SDF-1 alpha. *J Clin Invest.* 2007;117:1249-1259.
16. Hansen SL, Myers CA, Charboneau A, Young DM, Boudreau N. HoxD3 accelerates wound healing in diabetic mice. *Am J Pathol.* 2003;163:2421-2431.
17. Nanney LB, Wamil BD, Whitsitt J, Cardwell NL, Davidson JM, Yan HP, Hellerqvist CG. CM101 stimulates cutaneous wound healing through an anti-angiogenic mechanism. *Angiogenesis.* 2001;4:61-70.
18. Ebrahimian TG, Pouzoulet F, Squiban C, Buard V, Andre M, Cousin B, Gourmelon P, Benderitter M, Casteilla L, Tamarat R. Cell therapy based on adipose tissue-derived stromal cells promotes physiological and pathological wound healing. *Arterioscler Thromb Vasc Biol.* 2009;29:503-510.
19. Reynolds LE, Conti FJ, Silva R, Robinson SD, Iyer V, Rudling R, Cross B, Nye E, Hart IR, Dipersio CM, Hodivala-Dilke KM. alpha3beta1 integrin-controlled Smad7 regulates reepithelialization during wound healing in mice. *J Clin Invest.* 2008;118:965-974.
20. Ross C, Alston M, Bickenbach JR, Aykin-Burns N. Oxygen tension changes the rate of migration of human skin keratinocytes in an age-related manner. *Exp Dermatol.* 2010;20:58-63.
21. Schroder K, Kohnen A, Aicher A, Liehn EA, Buchse T, Stein S, Weber C, Dimmeler S, Brandes RP. NADPH oxidase Nox2 is required for hypoxia-induced mobilization of endothelial progenitor cells. *Circ Res.* 2009;105:537-544.